

Preparation and Characterization of $[\text{Hg}\{\text{P}(\text{C}_6\text{F}_5)_2\}_2]$, $[\text{Hg}\{\mu\text{-P}(\text{C}_6\text{F}_5)_2\text{W}(\text{CO})_5\}_2]$, and $[\text{Hg}\{\mu\text{-P}(\text{CF}_3)_2\text{W}(\text{CO})_5\}_2]$ and the X-ray Crystal Structure of $[\text{Hg}\{\mu\text{-P}(\text{C}_6\text{F}_5)_2\text{W}(\text{CO})_5\}_2]\cdot 2\text{DMF}$

Berthold Hoge,* Tobias Herrmann, Christoph Thösen, and Ingo Pantenburg

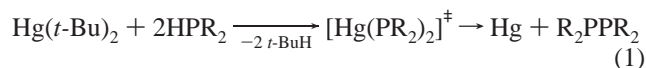
Institut für Anorganische Chemie, Universität zu Köln, D-50939 Köln, Germany

Received April 29, 2003

The thermally unstable compound $[\text{Hg}\{\text{P}(\text{C}_6\text{F}_5)_2\}_2]$ was obtained from the reaction of mercury cyanide and bis-(pentafluorophenyl)phosphane in DMF solution and characterized by multinuclear NMR spectroscopy. The thermally stable trinuclear compounds $[\text{Hg}\{\mu\text{-P}(\text{CF}_3)_2\text{W}(\text{CO})_5\}_2]$ and $[\text{Hg}\{\mu\text{-P}(\text{C}_6\text{F}_5)_2\text{W}(\text{CO})_5\}_2]$ are isolated and completely characterized. The higher order NMR spectra exhibiting multinuclear satellite systems have been sufficiently analyzed. $[\text{Hg}\{\mu\text{-P}(\text{CF}_3)_2\text{W}(\text{CO})_5\}_2]\cdot 2\text{DMF}$ crystallizes in the monoclinic space group $C2/c$ with $a = 2366.2(3)$ pm, $b = 1046.9(1)$ pm, $c = 104.0(1)$ pm, and $\beta = 104.01(1)^\circ$. Structural, NMR spectroscopic, and vibrational data prove a weak coordination of the two DMF molecules. Structural, vibrational, and NMR spectroscopic evidence is given for a successive weakening of the π back-bonding effect of the W–P bond in the order $[\text{W}(\text{CO})_5\text{PH}(\text{R})_2]$, $[\text{Hg}\{\mu\text{-P}(\text{R})_2\text{W}(\text{CO})_5\}_2]$, and $[\text{W}\{\text{P}(\text{R})_2\}(\text{CO})_5]^-$ with $\text{R}_f = \text{C}_6\text{F}_5$ and CF_3 . The π back-bonding effect of the W–C bonds increases vice versa.

Introduction

Diphosphanidomercury derivatives $[\text{Hg}(\text{PR}_2)_2]$ with $\text{R} = \text{C}_6\text{H}_5$, C_2H_5 , $i\text{-C}_3\text{H}_7$, and C_6H_{11} are thermally sensitive compounds and tend toward reductive elimination of elemental mercury and formation of the corresponding diphosphane derivatives. This decomposition pathway has been used to prepare diphosphanes in high yields according to eq 1.¹ Pure mercury compounds have not been obtained so far,



whereas homoleptic phosphanidomercury compounds with sterically demanding groups bonded to the phosphorus atom, such as $\text{R} = t\text{-Bu}$,^{1,2} SiMe_3 ,³ and SiPh_3 ,⁴ exhibit remarkable thermal stability.

Electron-withdrawing CF_3 groups bonded to the phosphorus atoms effect a stabilization of the mercury compounds,

allowing the complete NMR spectroscopic characterization of $[\text{Hg}\{\text{P}(\text{CF}_3)_2\}_2]$.^{5,6}

In a foregoing paper⁵ we described the stabilization of $[\text{Hg}\{\text{P}(\text{CF}_3)_2\}_2]$ in the presence of donor molecules such as phosphanes. While $[\text{Hg}\{\text{P}(\text{CF}_3)_2\}_2]$ decomposes slowly to elemental mercury and $(\text{CF}_3)_2\text{PP}(\text{CF}_3)_2$ at room temperature, the related phosphane adducts $[\text{Hg}\{\text{P}(\text{CF}_3)_2\}_2(\text{PR}_3)_2]$ ($(\text{PR}_3)_2 = (\text{PMe}_3)_2$, dppe) exhibit decomposition points at 157 and 147 °C, respectively.⁵

Another type of stabilization is observed, coordinating the phosphanido ligands to group VI metal carbonyl complexes.^{7,8} While $[\text{Hg}(\text{PPh}_2)_2]$ is unknown so far, Peringer et al. succeeded in the synthesis of the comparable trinuclear compound $[\text{Hg}\{\mu\text{-PPh}_2\text{M}(\text{CO})_5\}_2]$ with $\text{M} = \text{Cr}$, Mo , and W .⁸

Herein, we report the preparation of the novel bis(pentafluorophenyl)phosphanido derivative $[\text{Hg}\{\text{P}(\text{C}_6\text{F}_5)_2\}_2]$. The

* Author to whom correspondence should be addressed. Fax: 049-221-470-5196. E-mail: b.hoge@uni-koeln.de.

(1) Baudler, M.; Zarkadas, A. *Chem. Ber.* **1972**, *105*, 3844–3849.
 (2) Benac, B. L.; Cowley, A. H.; Jones, R. A.; Nunn, C. M.; Wright, T. C. *J. Am. Chem. Soc.* **1989**, *111*, 4986–4988.
 (3) Goel, S. C.; Chiang, M. Y.; Rauscher, C. D.; Buhro, W. E. *J. Am. Chem. Soc.* **1993**, *115*, 160–169.
 (4) Matchett, M. A.; Chiang, M. Y.; Buhro, W. E. *Inorg. Chem.* **1994**, *33*, 1109–1114.

(5) Hoge, B.; Thösen, C.; Pantenburg, I. *Inorg. Chem.* **2001**, *40*, 3084–3088.
 (6) Grobe, J.; Demuth, R. *Angew. Chem.* **1972**, *84*, 1153; *Angew. Chem., Int. Ed. Engl.* **1972**, *11*, 1097.
 (7) Eichbichler, J.; Malleier, R.; Wurst, K.; Peringer, P. *J. Organomet. Chem.* **1997**, *541*, 233–236. Obendorf, D.; Peringer, P. *J. Organomet. Chem.* **1987**, *326*, 375–380. Obendorf, D.; Peringer, P. *J. Organomet. Chem.* **1987**, *320*, 47–51. Peringer, P.; Lusser, M. *Inorg. Chim. Acta* **1986**, *117*, L25–L26.
 (8) Peringer, P.; Eichbichler, J. *J. Chem. Soc., Dalton Trans.* **1982**, 667–668.

Preparation of Diphosphanidomercury Derivatives

thermally sensitive compounds $[\text{Hg}\{\text{P}(\text{C}_6\text{F}_5)_2\}_2]$ and $[\text{Hg}\{\text{P}(\text{CF}_3)_2\}_2]$ are stabilized by the coordination of both phosphanido ligands to $\text{W}(\text{CO})_5$ moieties, forming the novel trinuclear complexes $[\text{Hg}\{\mu\text{-PR}_2\}\text{W}(\text{CO})_5\}_2]$ ($\text{R} = \text{C}_6\text{F}_5$ and CF_3).

Experimental Section

Materials and Apparatus. Chemicals were obtained from commercial sources and used without further purification. Literature methods were used for the synthesis of $\text{HP}(\text{C}_6\text{F}_5)_2$, $[\text{W}(\text{CO})_5\text{PH}(\text{C}_6\text{F}_5)_2]$, and $[\text{W}(\text{CO})_5\text{PH}(\text{CF}_3)_2]$.⁹ Solvents were purified by standard methods.¹⁰ Standard high-vacuum techniques were employed throughout all preparative procedures; nonvolatile compounds were handled in a dry N_2 atmosphere by using Schlenk techniques.

Infrared spectra were recorded on a Nicolet-5PC-FT-IR spectrometer using KBr pellets. Raman spectra were measured on a Bruker FRA-106/s spectrometer with a Nd:YAG laser operating at $\lambda = 1064$ nm.

NMR spectra were recorded on Bruker Model AMX 300 (^3P , 121.50 MHz; ^{19}F , 282.35 MHz) and Bruker AC200 (^3P , 81.01 MHz; ^{19}F , 188.31 MHz; ^1H , 200.13 MHz) spectrometers. Fluorine-decoupled phosphorus spectra were recorded on a Bruker DRX 500 spectrometer (^3P , 202.40 MHz) with positive shifts being downfield from the external standards (85% orthophosphoric acid (^3P), CCl_3F (^{19}F), and TMS (^1H)). Higher order NMR spectra were calculated with the program gNMR.¹¹

Preparation of $[\text{Hg}\{\mu\text{-P}(\text{C}_6\text{F}_5)_2\}\text{W}(\text{CO})_5\}_2\cdot 2\text{DMF}$. A solution of 0.28 g (1.11 mmol) of $\text{Hg}(\text{CN})_2$ in 5 mL of DMF was added dropwise to a solution of 1.63 g (2.37 mmol) of $[\text{W}(\text{CO})_5\text{PH}(\text{C}_6\text{F}_5)_2]$ in 5 mL of DMF at -50 °C. After the resulting solution was warmed to ambient temperature, the product $[\text{Hg}\{\mu\text{-P}(\text{C}_6\text{F}_5)_2\}\text{W}(\text{CO})_5\}_2\cdot 2\text{DMF}$ began to precipitate as yellow-green crystals. After precipitation was completed, the solvent was removed via a syringe and the residue was washed several times with diethyl ether and dried in vacuo. $[\text{Hg}\{\mu\text{-P}(\text{C}_6\text{F}_5)_2\}\text{W}(\text{CO})_5\}_2\cdot 2\text{DMF}$ (1.00 g, 0.58 mmol, 55%) is only moderately soluble in CH_2Cl_2 , CHCl_3 , and THF. The product loses the DMF solvent molecules at 105 °C (TG: mass loss 6%, calcd 8.5%). The resulting $[\text{Hg}\{\mu\text{-P}(\text{C}_6\text{F}_5)_2\}\text{W}(\text{CO})_5\}_2]$ decomposes at 175 °C (TG). Elemental analysis of $[\text{Hg}\{\mu\text{-P}(\text{C}_6\text{F}_5)_2\}\text{W}(\text{CO})_5\}_2\cdot 2\text{DMF}$ (calcd for $\text{C}_{40}\text{H}_{14}\text{F}_{20}\text{HgN}_2\text{O}_{12}\text{P}_2\text{W}_2$): N 1.79 (1.62); C 27.86 (27.15); H 0.82 (0.76). IR (cm^{-1} , KBr pellet): 2942 w, 2073 s, 1987 m, 1952 vs br, 1927 vs br, 1659 s, 1651s, 1520 s, 1470 s, 1414 vw, 1387 m, 1285 w, 1254 vw, 1138 vw, 1088 s, 1022 vw, 974 s, 839 w, 827 w, 764 vw, 752 vw, 721 vw, 667 w, 623 w, 598 m, 575 m, 505 w, 420 m. Raman (cm^{-1}): 2944 (13), 2073 (68), 1990 (100), 1950 (20), 1918 (72), 1642 (24), 1440 (6), 1414 (11), 1384 (19), 1286 (6), 1101 (5), 865 (7), 827 (28), 666 (4), 624 (4), 586 (27), 503 (13), 448 (64), 428 (56), 412 (34), 400 (38), 371 (15), 342 (66), 233 (6), 150 (15), 103 (100). MS $\{m/z$ (%) [assignment]: 1579 (<1) $[\text{HgP}_2(\text{C}_6\text{F}_5)_4\text{W}_2(\text{CO})_{10}]^+$; 1322 (4) $[\text{P}_2(\text{C}_6\text{F}_5)_4\text{W}_2(\text{CO})_8]^+$; 1294 (25) $[\text{P}_2(\text{C}_6\text{F}_5)_4\text{W}_2(\text{CO})_7]^+$; 1266 (2) $[\text{P}_2(\text{C}_6\text{F}_5)_4\text{W}_2(\text{CO})_6]^+$; 1255 (1) $[\text{HgP}_2(\text{C}_6\text{F}_5)_4\text{W}(\text{CO})_5]^+$; 1210 (3) $[\text{P}_2(\text{C}_6\text{F}_5)_4\text{W}_2(\text{CO})_4]^+$; 1182 (30) $[\text{P}_2(\text{C}_6\text{F}_5)_4\text{W}_2(\text{CO})_3]^+$; 1154 (4) $[\text{P}_2(\text{C}_6\text{F}_5)_4\text{W}_2(\text{CO})_2]^+$; 1126 (21) $[\text{P}_2(\text{C}_6\text{F}_5)_4\text{W}(\text{CO})]^+$; 1098 (32) $[\text{P}_2(\text{C}_6\text{F}_5)_4\text{W}]^+$; 730 (72) $[\text{P}_2(\text{C}_6\text{F}_5)_4]^+$; 365 (100) $[\text{P}$

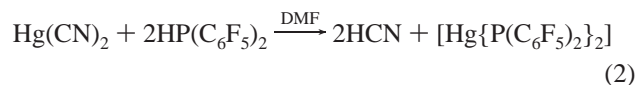
$(\text{C}_6\text{F}_5)_2]^+$; 73 (74) $[(\text{CH}_3)_2\text{NCOH}]^+$. NMR for $[\text{Hg}\{\mu\text{-P}(\text{C}_6\text{F}_5)_2\}\text{W}(\text{CO})_5\}_2]$ (saturated THF- d_8 solution; 298 K): $\delta(^3\text{P}) -74.4$ ppm; $\delta(^{19}\text{F}_o) -128.5$ ppm (m, 2F); $\delta(^{19}\text{F}_m) -160.0$ ppm (m, 2F); $\delta(^{19}\text{F}_p) -149.6$ ppm (m, 1F); $^1J(^{199}\text{HgP}) = 1864$ Hz; $^1J(^{183}\text{WP}) = 218$ Hz; $^2J(\text{PP}) = 137$ Hz.

Preparation of $[\text{Hg}\{\mu\text{-P}(\text{CF}_3)_2\}\text{W}(\text{CO})_5\}_2\cdot 2\text{DMF}$. A 0.93 g (1.89 mmol) sample of $[\text{W}(\text{CO})_5\text{PH}(\text{CF}_3)_2]$ and 0.20 g (0.80 mmol) of $\text{Hg}(\text{CN})_2$ were dissolved in 5 mL of DMF. After being stirred for 2 h at room temperature, the yellow solution was evaporated to dryness. The resulting intense yellow residue was washed once with 5 mL of CH_2Cl_2 and dried in vacuo, yielding 0.34 g (0.26 mmol, 33%) of $[\text{Hg}\{\mu\text{-P}(\text{CF}_3)_2\}\text{W}(\text{CO})_5\}_2\cdot 2\text{DMF}$ as a yellow powder. Elemental analysis of $[\text{Hg}\{\mu\text{-P}(\text{CF}_3)_2\}\text{W}(\text{CO})_5\}_2\cdot 2\text{DMF}$ (calcd for $\text{C}_{20}\text{H}_{14}\text{F}_{12}\text{HgN}_2\text{O}_{12}\text{P}_2\text{W}_2$): C 18.71 (18.03); H 1.23 (1.06); N 1.06 (2.10). IR (cm^{-1} , KBr pellet): 2943 w, 2082 s, 1955 vs, 1928 vs sh, 1650 s, 1386 w, 1175 s, 1124 s, 1064 vw, 994 vw, 931 vw, 742, vw, 670 w, 595 m, 571 m, 558 w sh, 550 w sh, 468 w, 457 vw sh, 434 w. Raman (cm^{-1}): 2946 (7), 2080 (85), 2010 (60), 1996 (60), 1961 (87), 1651 (5), 1149 (5), 1109 (4), 968 (10), 742 (25), 575 (8), 550 (28), 451 (55), 433 (100), 400 (32), 233 (64), 169 (34), 106 (90).

The product loses the DMF ligands in vacuo at room temperature, yielding $[\text{Hg}\{\mu\text{-P}(\text{CF}_3)_2\}\text{W}(\text{CO})_5\}_2]$. Elemental analysis of $[\text{Hg}\{\mu\text{-P}(\text{CF}_3)_2\}\text{W}(\text{CO})_5\}_2]$ (calcd for $\text{C}_{14}\text{F}_{12}\text{HgO}_{10}\text{P}_2\text{W}_2$): C 15.10 (14.17); H 0.02 (0.00); N 0.05 (0.00). A TG investigation exhibits no mass loss until the decomposition temperature of 200 °C is attained. MS $\{m/z$ (%) [assignment]: 1186 (60) $[\text{HgP}_2(\text{CF}_3)_4\text{W}_2(\text{CO})_{10}]^+$; 862 (18) $[\text{HgP}_2(\text{CF}_3)_4\text{W}(\text{CO})_5]^+$; 665 (15) $[\text{HgP}(\text{CF}_3)_2\text{W}(\text{CO})_4]^+$; 493 (75) $[\text{P}(\text{CF}_3)_2\text{W}(\text{CO})_5]^+$; 465 (64) $[\text{P}(\text{CF}_3)_2\text{W}(\text{CO})_4]^+$; 409 (29) $[\text{P}(\text{CF}_3)_2\text{W}(\text{CO})_2]^+$; 353 (8) $[\text{P}(\text{CF}_3)_2\text{W}]^+$; 315 (100) $[\text{W}(\text{CO})_4\text{F}]^+$; 303 (16) $[\text{P}(\text{CF}_3)\text{FW}]^+$; 287 (8) $[\text{W}(\text{CO})_3\text{F}]^+$; 284 (7) $[\text{P}(\text{CF}_3)\text{W}]^+$; 202 (10) $[\text{Hg}]^+$; 73 (19) $[(\text{CH}_3)_2\text{NCOH}]^+$. NMR for $[\text{Hg}\{\mu\text{-P}(\text{CF}_3)_2\}\text{W}(\text{CO})_5\}_2\cdot 2\text{DMF}$ (saturated CDCl_3 solution; 298 K): $\delta(^3\text{P}) 43.1$ ppm (m); $\delta(^{19}\text{F}) -48.8$ ppm (m); $^1J(^{199}\text{HgP}) = 2685$ Hz; $^1J(^{183}\text{WP}) = 217$ Hz; $^3J(^{199}\text{HgF}) = 105$ Hz; $^2J(\text{PP}) 111 =$ Hz; $^2J(\text{PF}) = 63.8$ Hz; $^4J(\text{PF}) = 2$ Hz. The ^1H NMR data of the DMF ligand molecule are not essentially influenced in comparison to those of noncoordinated DMF: $\delta(^1\text{H}) 7.9$ (1H); 3.0 (3H); 2.9 (3H) ppm.

Results and Discussion

The first preparation of a the bis(pentafluorophenyl)-phosphanidomercury compound exploits the weak acidity of HCN in the reaction of mercury cyanide with $\text{HP}(\text{C}_6\text{F}_5)_2$ at -30 °C in DMF solution:



The product $[\text{Hg}\{\text{P}(\text{C}_6\text{F}_5)_2\}_2]$ formed in a plain reaction exhibits no mercury satellites in the fluorine and phosphorus NMR spectra, which is caused through ligand exchange processes. All attempts to determine fluorine- and phosphorus-mercury coupling constants using different solvents and low temperatures have not been successful so far. The broad and temperature-dependent ^3P resonance of $[\text{Hg}\{\text{P}(\text{C}_6\text{F}_5)_2\}_2]$ is shifted by about 35 ppm to lower field with respect to the resonance of $\text{HP}(\text{C}_6\text{F}_5)_2$; cf. Table 1.

Caused by the stabilizing electron-withdrawing effect of the pentafluorophenyl groups, $[\text{Hg}\{\text{P}(\text{C}_6\text{F}_5)_2\}_2]$ decomposes slowly at room temperature, while the nonfluorinated deriva-

- (9) Hoge, B.; Herrmann, T.; Thösen, C.; Pantenburg, I. *Inorg. Chem.* **2003**, *42*, 3623–3632.
(10) Perrin, D. D.; Armarego, W. L. F.; Perrin, D. R. *Purification of Laboratory Chemicals*; Pergamon Press: Oxford, England, 1980.
(11) Budzelaar, P. H. M. *gNMR Version 4.1*; Chermwell Scientific: Oxford, U.K., 1998.

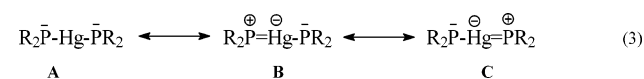
Table 1. Crystal Data and Structure Refinement Parameters for [Hg{(μ -P(C₆F₅)₂)₂W(CO)₅]₂·2DMF

empirical formula	C ₄₀ H ₁₄ F ₂₀ N ₂ O ₁₂ P ₂ W ₂ Hg	fw	1724.76
		Data Collection	
diffractometer	STOE IPDS II	exposure time (min)	7
radiation	Mo K α (graphite monochromator, $\lambda = 71.073$ pm)	detector distance (mm)	120
temp (K)	170(2)	2 θ range (deg)	1.9–54.8
index range	–26 $\leq h \leq$ +30 –13 $\leq k \leq$ +13 –26 $\leq l \leq$ +26	no. of total data collected	22263
rotation angle range	0° $\leq \omega \leq$ 180°; $\psi = 0^\circ$ 0° $\leq \omega \leq$ 70°; $\psi = 90^\circ$	no. of unique data	5408
increment	$\Delta\omega = 2^\circ$	no. of obsd data	3139
no. of images	125	R_{merg}	0.1030
		abs correction	numerical, after crystal shape optimization ^{20,21}
		transm max/min	0.2552/0.4306
		Crystallographic Data	
cryst size (mm)	0.2 \times 0.2 \times 0.1	β (deg)	104.01(1)
color, habit	yellow, column	vol (nm ³)	4.871(1)
cryst syst	monoclinic	Z	4
space group	C2/c (No. 15)	ρ_{calcd} (g cm ^{–3})	2.352
a (pm)	2366.2(3)	μ (mm ^{–1})	8.061
b (pm)	1046.9(1)	F(000)	3208
c (pm)	2026.4(3)	Structure Analysis and Refinement	
structure determination	SHELXS-97 ²² and SHELXL-93 ²³	GOF (S_{obsd}) ^b	0.939
no. of variables	360	GOF (S_{all}) ^b	0.802
R indexes ^a [$I > 2\sigma I$]	R1 = 0.0370 wR2 = 0.0428	largest difference map hole/peak (10 ^{–6} e pm ^{–3})	–2.050/1.173
R indexes ^a (all data)	R1 = 0.0891 wR2 = 0.0493		

^a $R1 = \sum(|F_o| - |F_c|)/\sum|F_o|$. $wR2 = [\sum w(|F_o|^2 - |F_c|^2)^2/\sum w(|F_o|^2)^2]^{1/2}$. ^b $S_2 = [\sum w(|F_o|^2 - |F_c|^2)^2/(n - p)]^{1/2}$, with $w = 1/[\sigma^2(F_o)^2 + (0.0027P)^2]$, where $P = (F_o^2 + 2F_c^2)/3$. $F_c^* = kF_c[1 + 0.001|F_c|^2\lambda^3/\sin(2\theta)]^{-1/4}$.

tive [Hg(PPh₂)₂] decomposes even at lower temperatures and cannot be obtained so far.¹ All attempts to isolate [Hg{P(C₆F₅)₂]₂] as a pure compound, removing the volatile compounds in vacuo, remain unsuccessful and lead to the reductive elimination of elemental mercury. The decomposition yields only minor amounts of (C₆F₅)PP(C₆F₅)₂ besides further unknown products.

Phosphanido–transition-metal complexes with less than 18 valence electrons show a phosphanido–phosphenium bonding dualism.^{12,13} As discussed previously, diphosphanidomercury compounds [Hg(PR₂)₂] may be described by the following resonance structures:⁵



The resonance structures **B** and **C** both contain a nucleophilic phosphorus atom and an electrophilic phosphorus atom.¹³ This approach explains why two phosphorus atoms smoothly combine with reductive elimination of elemental mercury.

This basic approach gives a qualitative description of the thermal stability of diphosphanidomercury derivatives with respect to a reductive elimination. If sterically demanding groups, such as R = *t*-Bu, SiMe₃, or SiPh₃, are attached to the phosphorus atoms, the resulting steric shielding of the phosphorus atoms prevents the combination of the PR₂ units: kinetical stabilization.

If strong electronegative groups are attached to the phosphorus atoms, the electron-withdrawing effect destabilizes the phosphenium bonding situation, i.e., destabilizes the formal positive charge at the phosphorus atom in the resonance structures **B** and **C**, resulting in a thermodynamical stabilization.

Theoretical calculations, using a partial retention of diatomic differential overlap (PRDDO) model, on different phosphanidotitanium derivatives, give evidence for a reduced phosphenium bonding contribution of (CF₃)₂P–Ti compounds with respect to comparable R₂P–Ti derivatives with R = H, CH₃, and C₆H₅.¹⁴ The calculations lead to elongated P–Ti distances and increased inversion barriers for the bis-(trifluoromethyl)phosphanido derivatives Cl₃TiPR₂, CpCl₂TiPR₂, and Cp₂CITiPR₂ with respect to nonfluorinated derivatives.

Another possibility to stabilize phosphanidomercury derivatives, which means to reduce the phosphenium bonding contribution (resonance structures **B** and **C**), is achieved by the formation of 18 valence electron complexes such as [Hg{P(CF₃)₂]₂(PR₃)₂] ((PR₃)₂ = (PMe₃)₂, dppe).⁵

Peringer et al.⁸ found that phosphanidomercury compounds can be stabilized if the phosphorus atoms are coordinated to low-valent transition-metal compounds, such as M(CO)₅ (M = Cr, Mo, W). Thus, the formally free phosphorus lone pairs are no longer accessible for the realization of a phosphenium bonding situation. The trinuclear compounds [Hg{(μ -PPh₂)M(CO)₅]₂], which are accessible via the reaction of [Hg{N(SiMe₃)₂]₂] and [M(CO)₅PHPh₂], show melting points above 140 °C.

(12) Collman, J. P.; Hegedus, L. S.; Norton, J. R.; Finke, R. G. *Principles and Application of Organotransition Metal Chemistry*; University Science Books: Mill Valley, CA, 1987.

(13) Baker, R. T.; Whitney, J. F.; Wreford, S. S. *Organometallics* **1983**, *2*, 1049–1051.

(14) Rogers, J. R.; Wagner, T. P. S.; Marynick, D. S. *Inorg. Chem.* **1994**, *33*, 3104–3110 and references cited therein.

Table 2. NMR Spectroscopic Data for Bis(pentafluorophenyl)phosphorus Derivatives^a

	$\delta(^{31}\text{P})$	$\delta(^{19}\text{F}_o)$	$\delta(^{19}\text{F}_m)$	$\delta(^{19}\text{F}_p)$	$^1J(\text{PH})$	$^1J(\text{PW})$	$^1J(\text{HgP})$	$^2J(\text{PP})$
$\text{HP}(\text{C}_6\text{F}_5)_2^9$	-137.7	-128.3	-159.6	-149.3	236.5			
$[\text{Hg}\{\text{P}(\text{C}_6\text{F}_5)_2\}_2]^b$	-102.9	-127.2	-162.9	-154.7			nr	
$[\text{W}\{\text{P}(\text{C}_6\text{F}_5)_2\}(\text{CO})_5]^{18}$	-103.9	-127.9	-165.2	-162.7		99.5		
$[\{\text{W}(\text{CO})_5\}_2\{\mu\text{-P}(\text{C}_6\text{F}_5)_2\}]^{18}$	-111.5	-125.1	-163.5	-159.1		172.8		
$[\text{Hg}\{\mu\text{-P}(\text{C}_6\text{F}_5)_2\}\text{W}(\text{CO})_5]_2^c$	-74.4	-128.5	-160.0	-149.6		218	1864	137
$[\text{W}(\text{CO})_5\text{PH}(\text{C}_6\text{F}_5)_2]^9$	-100.1	-131.2	-160.3	-148.5	380.5	249.9		

^a nr = not resolved. ^b DMF, 298 K. ^c See the Experimental Section.

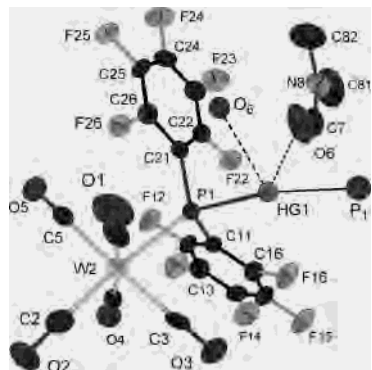


Figure 1. Central projection of the asymmetric unit of $[\text{Hg}\{\mu\text{-P}(\text{C}_6\text{F}_5)_2\}\text{W}(\text{CO})_5\}_2] \cdot 2\text{DMF}$ showing the atom numbering scheme and thermal ellipsoids (50%).

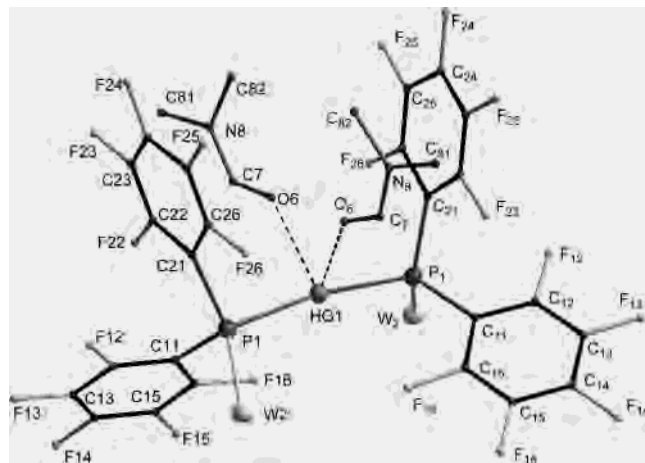
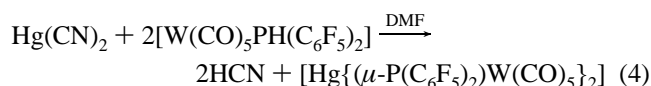


Figure 2. Simplified view of $[\text{Hg}\{\mu\text{-P}(\text{C}_6\text{F}_5)_2\}\text{W}(\text{CO})_5\}_2] \cdot 2\text{DMF}$. The CO groups have been omitted for clarity. A subscript atom identifier indicates symmetry-dependent atoms.

Mercury cyanide smoothly reacts with a slight excess of $[\text{W}(\text{CO})_5\text{PH}(\text{C}_6\text{F}_5)_2]$ at $-50\text{ }^\circ\text{C}$ to give the trinuclear compound $[\text{Hg}\{\mu\text{-P}(\text{C}_6\text{F}_5)_2\}\text{W}(\text{CO})_5\}_2]$:



The product crystallizes, with two DMF solvent molecules, from the reaction mixture on warming to room temperature. The crystal data and structure refinement parameters for $[\text{Hg}\{\mu\text{-P}(\text{C}_6\text{F}_5)_2\}\text{W}(\text{CO})_5\}_2] \cdot 2\text{DMF}$ are given in Table 2. The asymmetric unit of the C_2 symmetric complex with the atom numbering scheme is shown in Figure 1, whereas Figure 2 exhibits a simplified view of the trinuclear complex, the CO groups having been omitted for clarity. Selected bond lengths and angles are summarized in Table 3.

Table 3. Selected Bond Lengths (pm) and Angles (deg) for $[\text{Hg}\{\mu\text{-P}(\text{C}_6\text{F}_5)_2\}\text{W}(\text{CO})_5\}_2] \cdot 2\text{DMF}$

Hg1–P1	244.2(2)	P1–Hg1–P1'	170.25(9)
Hg1–O6	255.3(6)	P1–Hg1–O6	91.1(2)
W2–C2	199.0(9)	P1–Hg1–O6'	96.2(2)
W2–C4	200.1(9)	O6–Hg1–O6'	82.7(3)
W2–C1	200.2(9)	C4–W2–P1	174.5(3)
W2–C3	203.6(9)	C4–W2–P1	91.8(2)
W2–C5	204.9(9)	C1–W2–P1	92.6(2)
W2–P1	254.4(2)	C3–W2–P1	83.8(2)
P1–C11	184.5(7)	C5–W2–P1	92.8(2)
P1–C21	184.7(7)	C11–P1–C21	103.1(3)
C11–C12	137(1)	C11–P1–Hg1	107.6(2)
C11–C16	138(1)	C21–P1–Hg1	99.9(2)
C12–F12	135.6(8)	C11–P1–W2	106.0(2)
C12–C13	138(1)	C21–P1–W2	122.6(2)
C15–F15	135.0(8)	Hg1–P1–W2	116.33(7)
C15–C16	138.2(9)	C7–O6–Hg1	140.5(7)
C16–F16	135.5(8)	O6–C7–N8	126(1)
O6–C7	120(1)	C7–N8–C81	123.1(9)
C7–N8	131(1)	C7–N8–C82	120.9(8)
N8–C81	145.4(9)	C81–N8–C82	116.0(8)

Although we obtain a 4-fold coordination of the mercury atom, the P–Hg–P unit exhibits a nearly linear arrangement. One reason for the linear arrangement may be the bulkiness of the two sterically demanding phosphanido substituents. But if compared with complexes of urea derivatives with mercury(II) chloride, $[\text{HgCl}_2\text{D}_2]$, which also exhibit a nearly linear Cl–Hg–Cl arrangement,¹⁵ the smaller coordination strength of the amide ligands seems to be responsible for the nearly linear P–Hg–P arrangement shown in Figure 2.

The DMF ligands are coordinated via the oxygen atom, and the CO distance is therefore elongated by around 3 pm in comparison with that of solid DMF.¹⁶ The CO valence mode cannot be assigned with absolute certainty because the C_6F_5 groups exhibit a strong CC valence mode in both the infrared and Raman spectra. The latter exhibits a medium intense band at 1642 cm^{-1} which is assigned to a CC valence mode because this resonance shows the same intensity as observed for previously investigated pentafluorophenylphosphorus derivatives.⁹ The CO valence mode of DMF shows only a weak Raman intensity. In the infrared spectrum two strong resonances are detected at 1659 and 1651 cm^{-1} . Following the assignment of the Raman resonance, we assign the resonance at 1659 cm^{-1} to the CO valence mode of the DMF ligand, which is shifted about 50 cm^{-1} to lower frequencies in comparison to that of gaseous DMF¹⁷ but

(15) Lewinski, K.; Sliwinski, J.; Lebioda, L. *Inorg. Chem.* **1983**, *22*, 2339–2342. Birker, P. J. M. W. L.; Freeman, H. C.; Guss, J. M.; Watson, A. D. *Acta Crystallogr.* **1977**, *B33*, 182–184. Majeste, R. J.; Trefonas, L. M. *Inorg. Chem.* **1972**, *11*, 1834–1836.

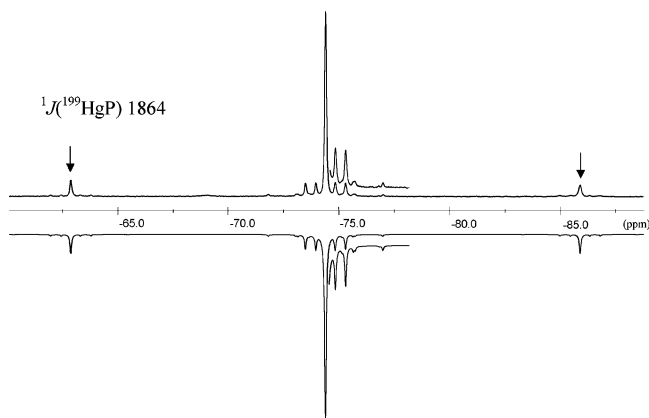
(16) Borrmann, H.; Persson, I.; Sandström, M.; Stålhandske, C. M. V. *J. Chem. Soc., Perkin Trans. 2* **2000**, 393–402.

(17) Jao, T. C.; Scott, I.; Steele, D. *J. Mol. Spectrosc.* **1982**, *92*, 1–17.

Table 4. $^1J(\text{PW})$ and the Highest Infrared CO Valence Mode of Bis(pentafluorophenyl)phosphorus Derivatives Coordinated to a Pentacarbonyltungsten Ion in Comparison to Their Structural Data

	$^1J(\text{PW})$ (Hz)	$d(\text{WP})$ (pm)		$\nu(\text{CO})^a$ (cm^{-1})	$d(\text{WC}_{\text{tr}})$ (pm)	
		X-ray	calcd ^b		X-ray	calcd ^b
$[\text{W}(\text{CO})_5\text{PH}(\text{C}_6\text{F}_5)_2]^9$	249.9	247.7(1)	250.5	2084	201.1(6)	201.1
$[\text{Hg}\{\mu\text{-P}(\text{C}_6\text{F}_5)_2\}\text{W}(\text{CO})_5\}_2] \cdot 2\text{DMF}$	217.8	254.4(2) ^c		2073	199.0(9) ^c	
$[\text{W}\{\text{P}(\text{C}_6\text{F}_5)_2\}(\text{CO})_5]^-^{18}$	99.5		266.4	2054		198.4

^a Highest infrared CO valence mode. ^b B3PW91 with a LanL2DZ ECP basis for tungsten and a 6-311G(d,p) basis for the nonmetal atoms. ^c X-ray data of $[\text{Hg}\{\mu\text{-P}(\text{C}_6\text{F}_5)_2\}\text{W}(\text{CO})_5\}_2] \cdot 2\text{DMF}$.

**Figure 3.** Experimental (top) and calculated (bottom) ^{31}P NMR spectrum of $[\text{Hg}\{\mu\text{-P}(\text{C}_6\text{F}_5)_2\}\text{W}(\text{CO})_5\}_2] \cdot 2\text{DMF}$.

exhibits nearly the same frequency as that of solid or liquid DMF, which is associated via $\text{C}-\text{H}\cdots\text{O}$ interactions.¹⁶

The Hg–P distance of 244 pm is comparable to those observed for $[\text{Hg}\{\text{P}(t\text{-Bu})_2\}_2]$, 244 and 245 pm, and $[\text{Hg}\{\text{P}(\text{SiMe}_3)_2\}_2]$, 240 and 241 pm. However, the phosphane complex $[\text{Hg}\{\text{P}(\text{CF}_3)_2\}_2\text{dppe}]$ exhibits phosphanido–mercury distances which are elongated by about 5 pm.⁵

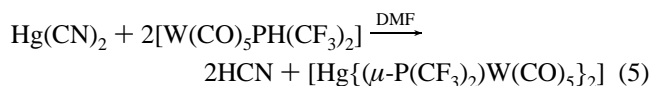
The W–P distance of 254 pm is elongated in comparison to that of the phosphane complex $[\text{W}(\text{CO})_5\text{PH}(\text{C}_6\text{F}_5)_2]$,⁹ 248 pm (X-ray) and 250 pm (DFT calculation). The distance is shortened in comparison to that of the phosphanido complex $[\text{W}\{\text{P}(\text{C}_6\text{F}_5)_2\}(\text{CO})_5]^-$, 266 pm (HDFT calculation).¹⁸ These findings are reasonable because a successive increase of electron density at the phosphorus atoms in the series $[\text{W}(\text{CO})_5\text{PH}(\text{C}_6\text{F}_5)_2]$, $[\text{Hg}\{\mu\text{-P}(\text{C}_6\text{F}_5)_2\}\text{W}(\text{CO})_5\}_2] \cdot 2\text{DMF}$, and $[\text{W}\{\text{P}(\text{C}_6\text{F}_5)_2\}(\text{CO})_5]^-$ has to be expected. As a consequence, the π acidity should decrease. As outlined in Table 3, this decrease of π acidity causes a shift of the highest symmetric CO valence mode to lower frequencies, indicating an increased π back-bonding effect of the CO groups as can be observed by means of the successive shortening of the WC distance of the *trans*-orientated CO group in the same series, Table 4.

The experimental ^{31}P NMR spectrum of $[\text{Hg}\{\mu\text{-P}(\text{C}_6\text{F}_5)_2\}\text{W}(\text{CO})_5\}_2] \cdot 2\text{DMF}$ is shown in Figure 3. The fluorine–phosphorus couplings are very small and could not be resolved. The major signal is surrounded by mercury satellites with a HgP coupling of 1864 Hz. The isotopomer of the W–P–Hg–P–W unit with one NMR-active ^{183}W

isotope gives rise to a magnetic nonequivalence of the two phosphorus atoms. The theoretical chemical difference of the two phosphorus atoms, caused by the isotopic shift, can be neglected in this case. The calculation of the resulting AA'X spin system ($[\text{A}]_2\text{X}$) with $\text{A} = \text{P}$ and $\text{X} = ^{183}\text{W}$ (bottom trace of Figure 3) allows the determination of the $^2J(\text{PP})$ coupling of 137 Hz.

The calculated ^{31}P NMR spectrum shown at the bottom trace of Figure 3 takes into account the mercury satellites, the tungsten satellites, and the $[\text{AX}]_2$ spin system for the isotopomer with two NMR-active ^{183}W isotopes in the W–P–Hg–P–W unit.

Mercury cyanide reacts smoothly with $[\text{W}(\text{CO})_5\text{PH}(\text{CF}_3)_2]$, yielding the corresponding trinuclear bis(trifluoromethyl)phosphanido compound $[\text{Hg}\{\mu\text{-P}(\text{CF}_3)_2\}\text{W}(\text{CO})_5\}_2]$:



After evaporation of the intense yellow solution to dryness, the powdery product is obtained as an adduct with two solvent molecules of DMF, which can be removed on extended evaporation of the crushed powder at room temperature.

In contrast to $[\text{Hg}\{\text{P}(\text{CF}_3)_2\}_2]$, which slowly decomposes at room temperature, the solvent-free compound $[\text{Hg}\{\mu\text{-P}(\text{CF}_3)_2\}\text{W}(\text{CO})_5\}_2]$ decomposes above 200 °C. The decomposition temperature lies more than 50 °C above the decomposition point of the comparable phosphane complexes $[\text{Hg}\{\text{P}(\text{CF}_3)_2\}_2(\text{PR}_3)_2]$ with $(\text{PR}_3)_2 = (\text{PMe}_3)_2$ and dppe.⁵

The DMF solvent molecules exhibit only weak interaction with the trinuclear complex, as is indicated by the removability of the solvent molecules in vacuo at room temperature. Further evidence for a merely weak interaction is outlined by the dynamic behavior in solution. The ^1H NMR resonances of the DMF moieties of the compound $[\text{Hg}\{\mu\text{-P}(\text{CF}_3)_2\}\text{W}(\text{CO})_5\}_2] \cdot 2\text{DMF}$ dissolved in CDCl_3 exhibit no significant difference in comparison to those of a diluted DMF solution in CDCl_3 .

The CO valence mode of the DMF molecule of solid $[\text{Hg}\{\mu\text{-P}(\text{CF}_3)_2\}\text{W}(\text{CO})_5\}_2] \cdot 2\text{DMF}$, located at 1651 cm^{-1} in the Raman spectrum and at 1650 cm^{-1} in the infrared spectrum, is shifted by more than 60 cm^{-1} to lower frequencies in comparison to that of DMF in the gas phase.¹⁷ On the other hand, C–H \cdots O-associated solid and liquid DMF exhibits no significant shift of the CO valence mode.¹⁶ The highest symmetric CO valence mode of 2082 cm^{-1} (IR) and 2080 cm^{-1} (RA) is shifted about 10 cm^{-1} to higher frequencies in comparison to the corresponding resonance of the pentafluorophenyl derivative $[\text{Hg}\{\mu\text{-P}(\text{C}_6\text{F}_5)_2\}\text{W}(\text{CO})_5\}_2] \cdot 2\text{DMF}$. The stronger electron-withdrawing effect of the CF_3 increases the π back-bonding effect of the P–W bond and therefore decreases the π back-bonding effect of the W–C bonds, which is indicated by the shift of the CO valence modes to higher frequencies.

The highest CO mode of the series $[\text{W}(\text{CO})_5\text{PH}(\text{CF}_3)_2]$, $[\text{Hg}\{\mu\text{-P}(\text{CF}_3)_2\}\text{W}(\text{CO})_5\}_2] \cdot 2\text{DMF}$, and $[\text{W}\{\text{P}(\text{CF}_3)_2\}(\text{CO})_5]^-$

(18) Hoge, B.; Thösen, C.; Herrmann, T. *Inorg. Chem.* **2003**, *42*, 3633–3641.

Table 5. NMR Spectroscopic Data for Bis(trifluoromethyl)-phosphorus Derivatives

	$\delta(^{31}\text{P})$	$\delta(^{19}\text{F})$	$^2J(\text{PF})$	$^1J(\text{PH})$	$^1J(\text{HgP})$	$^1J(\text{PW})$	$^2J(\text{PP})$
$\text{HP}(\text{CF}_3)_2$ ⁹	-48.0	-47.3	60.6	240.7			
$\text{P}(\text{CF}_3)_2$ ⁻²⁴	-1.9	-31.4	47.2				
$[\text{Hg}\{\text{P}(\text{CF}_3)_2\}_2(\text{dppe})]^{5-}$	-5.2	-39.4	54		623		
$[\text{Hg}\{\text{P}(\text{CF}_3)_2\}_2]^{5-}$	1.8	-39.8	54.2		823		12
$[\text{W}\{\text{P}(\text{CF}_3)_2\}_2(\text{CO})_5]^{-18}$	15.0	-42.8	50.1			103.1	
$[\text{Hg}\{\mu\text{-P}(\text{CF}_3)_2\}_2\text{W}(\text{CO})_5]^{19}$	43.1	-48.8	63.8		2685	217	111
$[\text{W}(\text{CO})_5\text{PH}(\text{CF}_3)_2]^{19}$	1.7	-54.9	75.9	359.5		268.8	

^a See the Experimental Section. $^3J(^{199}\text{HgF}) = 105$ Hz. $^4J(\text{PF}) = 2$ Hz.

shows the expected successive shift to lower frequencies of about 2093, 2081, and 2065 cm^{-1} , respectively.^{9,18} These frequencies describe an increasing π back-bonding effect of the W–C bond in this series, while the π back-bonding effect of the W–P bond increases vice versa.

Further support for an increasing π back-bonding effect of the W–P bond in the order $[\text{W}\{\text{P}(\text{CF}_3)_2\}_2(\text{CO})_5]^-$, $[\text{Hg}\{\mu\text{-P}(\text{CF}_3)_2\}_2\text{W}(\text{CO})_5]_2 \cdot 2\text{DMF}$, and $[\text{W}(\text{CO})_5\text{PH}(\text{CF}_3)_2]$ is given by the successively increased magnitude of the $^1J(^{183}\text{WP})$ coupling of 103, 214, and 269 Hz, respectively (Table 5).

The fluorine-decoupled ^{31}P NMR spectrum of $[\text{Hg}\{\mu\text{-P}(\text{CF}_3)_2\}_2\text{W}(\text{CO})_5]_2 \cdot 2\text{DMF}$ dissolved in CDCl_3 exhibits the same habit as is observed for the C_6F_5 derivative; cf. Figure 3. The observed $^1J(\text{HgP})$ coupling of 2685 Hz varies less than 10% when determined for the solvent adducts $[\text{Hg}\{\mu\text{-P}(\text{CF}_3)_2\}_2\text{W}(\text{CO})_5]_2 \cdot 2\text{D}$ with $\text{D} = \text{CH}_3\text{CN}$, diglyme, and DMF. As a result of ligand exchange phenomena the $^1J(\text{HgP})$ coupling of the pyridine and DMSO adducts could not be determined. These results are in contrast to the drastic changes in the $^1J(\text{HgP})$ coupling constant of the trinuclear compounds $[\text{Hg}\{\mu\text{-P}(\text{Ph})_2\}_2\text{M}(\text{CO})_5]_2$ with $\text{M} = \text{Cr}, \text{Mo},$ and W on coordination of neutral N and O ligands.¹⁹

As a result of the $^2J(\text{PF})$ and $^4J(\text{PF})$ couplings of 63.8 and 2 Hz, respectively, the fluorine-coupled ^{31}P NMR spectrum of $[\text{Hg}\{\mu\text{-P}(\text{CF}_3)_2\}_2\text{W}(\text{CO})_5]_2$ gives rise to a magnetic nonequivalence of the two $\text{P}(\text{CF}_3)_2$ units. This allows the determination of the $^2J(\text{PP})$ coupling by the calculation of the center signal as a $\text{A}_6\text{A}'_6\text{XX}'$ or $[\text{A}_6\text{X}]_2$ spin system, respectively (bottom of Figure 4). The determined value of 111 Hz matches exactly with the value obtained via the calculation of the tungsten satellites of the fluorine-decoupled phosphorus spectrum. The ^{199}Hg satellites, not shown in Figure 4, exhibit the same habit as the center signal. If the tungsten satellites are taken into account, the calculated ^{31}P NMR spectrum (bottom of Figure 4) is the sum of 85.72% of an $[\text{A}_6\text{X}]_2$ spin system and 14.28% of an $[\text{A}_6\text{X}]_2\text{M}$ spin system ($\text{A} = \text{F}; \text{X} = \text{P}; \text{M} = ^{183}\text{W}$). The experimental ^{19}F NMR spectrum is shown in the upper trace of Figure 5

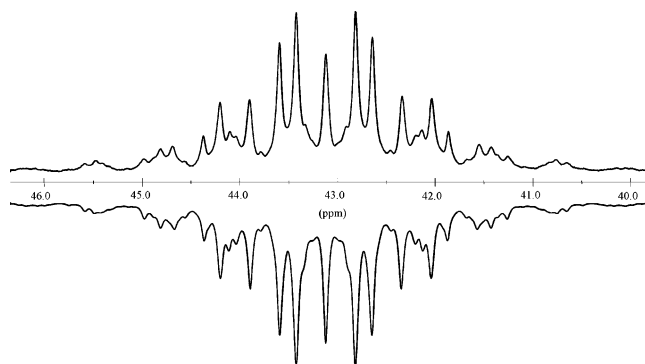


Figure 4. Experimental (top) and calculated (bottom) ^{31}P NMR spectrum of $[\text{Hg}\{\mu\text{-P}(\text{CF}_3)_2\}_2\text{W}(\text{CO})_5]_2 \cdot 2\text{DMF}$.

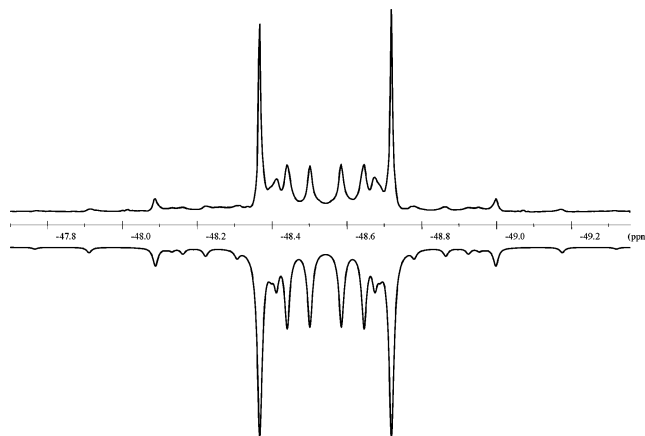


Figure 5. Experimental (top) and calculated (bottom) ^{19}F NMR spectrum of $[\text{Hg}\{\mu\text{-P}(\text{CF}_3)_2\}_2\text{W}(\text{CO})_5]_2 \cdot 2\text{DMF}$.

together with the calculated spectrum in the bottom trace of Figure 5 with respect to the ^{199}Hg satellites. The tungsten satellites could not be resolved in the fluorine NMR spectrum.

In previous papers we provided vibrational and X-ray structural evidence, supported by hybrid DFT calculations, that the electronic properties of the phosphanide ions $\text{P}(\text{CF}_3)_2^-$ and $\text{P}(\text{C}_6\text{F}_5)_2^-$ and of the comparable phosphanes $\text{HP}(\text{CF}_3)_2$ and $\text{HP}(\text{C}_6\text{F}_5)_2$ are not significantly influenced on coordination to a $\text{W}(\text{CO})_5$ unit.^{9,18} For example, the bis-(trifluoromethyl)phosphanidotungstate ion, $[\text{W}\{\text{P}(\text{CF}_3)_2\}_2(\text{CO})_5]^-$, exhibits nearly the same nucleophilicity as the noncoordinated $\text{P}(\text{CF}_3)_2^-$ ion. This finding can be described by the strong π acidity of perfluoroorganylphosphorus derivatives, which compensates the electron transfer via the σ donation from the phosphorus atom to the tungsten atom. As a consequence, complexation by pentacarbonyl group VI metals shows no significant influence on the structural and vibrational data of perfluoroorganylphosphorus derivatives, as is impressively demonstrated by the P–C distances of the $\text{P}(\text{CF}_3)_2^-$ and the $[\text{W}\{\text{P}(\text{CF}_3)_2\}_2(\text{CO})_5]^-$ ions.

Negative hyperconjugation of the $\text{P}(\text{CF}_3)_2^-$ ion leads to a significantly shortened P–C distance (C_2 symmetry) in comparison to those of neutral phosphane derivatives. Because of the weak influence on coordination to a $\text{W}(\text{CO})_5$ unit, the $[\text{W}\{\text{P}(\text{CF}_3)_2\}_2(\text{CO})_5]^-$ ion exhibits the same P–C distance within the measurement accuracy.

(19) Peringer, P. *Polyhedron* **1982**, *1*, 819–820.

(20) X-RED 1.22, *STOE Data Reduction Program*; Darmstadt, Germany, 2001.

(21) X-SHAPE 1.06, *Crystal Optimisation for Numerical Absorption Correction*; Darmstadt, Germany, 1999.

(22) Sheldrick, G. M. *SHELXS-97, Program for Crystal Structure Analysis*; University of Göttingen: Göttingen, Germany, 1998.

(23) Sheldrick, G. M. *SHELXL-93, Program for the Refinement of Crystal Structures*, University of Göttingen: Göttingen, Germany, 1993.

(24) Hoge, B.; Thösen, C. *Inorg. Chem.* **2001**, *40*, 3113–3116.

The increased stability of $[\text{Hg}\{\mu\text{-P}(\text{R})_2\text{W}(\text{CO})_5\}_2]$ with $\text{R} = \text{CF}_3$ and C_6F_5 in comparison to the noncoordinated monometallic counterpart is therefore interpretable in terms of a reduced phosphonium bonding contribution (resonance structures **B** and **C**). If the reductive elimination of mercury were interpretable in terms of a “classical” redox process, the coordination of the $\text{P}(\text{CF}_3)_2$ and $\text{P}(\text{C}_6\text{F}_5)_2$ ligands to a $\text{W}(\text{CO})_5$ unit would not lead to the observed strong increase in thermal stability.

Acknowledgment. We are grateful to Prof. Dr. D. Naumann for his generous support and the Fonds der Chemischen Industrie for financial support. We thank Dr. W. Tyrra and Dr. K. Glinka for helpful discussions.

Supporting Information Available: A crystallographic file in CIF format for $[\text{Hg}\{\mu\text{-P}(\text{C}_6\text{F}_5)_2\text{W}(\text{CO})_5\}_2]\cdot 2\text{DMF}$. This material is available free of charge via the Internet at <http://pubs.acs.org>. IC034448N